Journal of the Arkansas Academy of Science

Volume 65 Article 11

2011

# Boundary Condition on Electron Temperature for Antiforce Current Bearing Waves

M. Hemmati
*Arkansas Tech University*, mhemmati@atu.edu

W. P. Childs
*Arkansas Tech University*

D. C. Waters
*Arkansas Tech University*

J. D. Counts
*Arkansas Tech University*

J. K. Schmitt
*Arkansas Tech University*

# Boundary Condition on Electron Temperature for Antiforce Current Bearing Waves

M. Hemmati[1], W.P. Childs, D.C. Waters, J.D. Counts and J.K. Schmitt

[1]*Departmant of Physical Science, Arkansas Tech University, Russellville, AR 72801*

[1] Correspondence: mhemmati@atu.edu

**Abstract**

In our investigation of breakdown waves, we apply a one-dimensional, three-component, steady-state fluid model. The wave is considered to be shock fronted and the electrons are assumed to be the main element in propagation of the wave. In our fluid model, the electron gas temperature is assumed to be large enough to sustain the wave motion. Our set of fluid equations is composed of the equations of conservation of mass, momentum and energy plus the Poisson's equation.

This investigation involves breakdown waves for which a large current exist in the vicinity of the wave front. Existence of current behind the wave front alters the equation of conservation of energy and also the Poisson's equation. Therefore, the boundary conditions at the shock front will change as well. For current bearing breakdown waves we will derive the appropriate boundary condition for electron temperature, and using the new boundary condition, we will integrate the fluid dynamical equations through the dynamical transition region of the wave.

## Introduction

Paxton and Fowler (1962) considered the luminous pulses to be of fluid-dynamical nature and at the same time as Haberstich (1964) from the University of Maryland proposed a fluid model to describe luminous pulse propagation. Paxton and Fowler (1962) assumed the electrical breakdown wave front to be an electron shock wave and proposed a three-fluid, quasi-steady, hydro-dynamical model. They considered the electron gas partial pressure behind the shock front to be the main cause of the wave propagation. They derived a set of steady-state equations of conservation of mass, momentum, and energy transfer for a continuous medium.

Shelton and Fowler (1968) expanded Paxton's (1962) equations by introducing additional terms to the equations of conservation of momentum and energy. Also, they derived equations for momentum and energy loss terms during the electrons' collisions with heavy particles. Considering waves propagation into a neutral media (no magnetic field), and no time variation in the wave frame, the Maxwell's equations reduce to Poisson's equation alone. Therefore, they formulated a set of one-dimensional, steady-state, constant velocity electron fluid dynamical equations describing breakdown waves propagating into a non-ionized medium. Shelton and Fowler (1968) proposed the existence of two distinct regions. Following the shock front, they proposed existence of a thin dynamical region in which the electrons come to rest relative to heavy particles and the net electric field rapidly falls to a negligible value. They described this region as the sheath region. The sheath region is followed by a thicker region in which the ionization continues and the electron gas cools down to room temperature. Shelton (1968) referred to this region as the quasi-neutral region. Using an approximation method, Shelton and Fowler (1968) solved their set of electron fluid-dynamical equations for breakdown waves propagating into a neutral medium.

In 1984, Fowler et al. (1984) made significant contributions in completing Shelton's (1968) set of electron-fluid dynamical equations. They introduced three additional terms to the equation of conservation of energy in which the heat conduction term proved to be the most important one. In their attempt for numerical solution of the set of equations, they allowed for a discontinuity in the electron temperature derivative at the shock front, which significantly altered the conditions at the shock front. For breakdown waves propagating into a neutral medium, using the new set of boundary conditions, they successfully integrated the set of electron fluid-dynamical equations through the sheath region of the wave.

## Model

Breakdown waves for which the electric field force on electrons causes the average drift velocity of the electrons to be away from the wave front are referred to as antiforce waves. In the case of antiforce waves, the electron fluid pressure is considered to be large enough to provide the driving force and cause the

propagation of the wave down the tube with observed velocities.

To analyze breakdown waves, the equations that were developed by Fowler et al. (1984) and represent a one-dimensional, steady-state, electron fluid-dynamical wave propagating into a neutral medium at constant velocity will be used. These electron fluid-dynamical equations are the equations of conservation of mass, momentum, and energy coupled with Poisson's equation:

$$\frac{d(n\upsilon)}{dx} = n\beta, \qquad [1]$$

$$\frac{d}{dx}[mn\nu(\upsilon - V) + nkT_e] = -enE - Kmn(\upsilon - V), \qquad [2]$$

$$\frac{d}{dx}[mn\upsilon(\upsilon - V)^2 + nkT_e(5\upsilon - 2V) + 2en\upsilon\Phi$$

$$-\frac{5nk^2T_e}{mK}\frac{dT_e}{dx}] =$$

$$-3(\frac{m}{M})nkKT_e - (\frac{m}{M})Kmn(\upsilon - V)^2, \qquad [3]$$

$$\frac{dE}{dx} = \frac{e}{\varepsilon_0}n(\frac{\nu}{V} - 1). \qquad [4]$$

where $n, \nu, T_e, e$ and $m$ represent the electron number density, velocity, temperature, charge, and mass, respectively, and $M, E, E_0, V, k, K, x, \beta,$ and $\phi$ represent the neutral particle mass, electric field within the sheath region, electric field at the wave front, wave velocity, Boltzmann's constant, elastic collision frequency, position within the sheath region, ionization frequency and ionization potential of the gas.

Reducing the set of electron fluid dynamical equations to a non-dimensional form requires introduction of the following dimensionless variables:

$$\eta = \frac{E}{E_o}, \nu = (\frac{2e\phi}{\varepsilon_o E_o^2})n, \psi = \frac{\nu}{V}, \theta = \frac{T_e k}{2e\phi}, \xi = \frac{eE_o x}{mV^2},$$
$$\alpha = \frac{2e\phi}{mV^2}, \kappa = \frac{mV}{eE_o}K, \mu = \frac{\beta}{K}, \omega = \frac{2m}{M},$$

in which $\eta, \nu, \psi, \theta, \mu,$ and $\xi$ represent the dimensionless net electric field of the applied field plus the space charge field, electron number density, electron velocity, electron gas temperature, ionization rate, and position within the sheath region, while $\alpha$ and $\kappa$ represent wave parameters. These dimensionless variables are then substituted into equations 1, 2, 3 and 4, yielding

$$\frac{d(\nu\psi)}{d\xi} = \kappa\mu\nu, \qquad [5]$$

$$\frac{d}{d\xi}[\nu\psi(\psi - 1) + \alpha\nu\theta] = -\nu\eta - \kappa\nu(\psi - 1), \qquad [6]$$

$$\frac{d}{d\xi}[\nu\psi(\psi - 1)^2 + \alpha\nu\theta(5\psi - 2) + \alpha\nu\psi + \alpha\eta^2 -$$

$$\frac{5\alpha^2\nu\theta}{\kappa}\frac{d\theta}{d\xi}] = -\omega\kappa\nu[3\alpha\theta + (\psi - 1)^2], \qquad [7]$$

$$\frac{d\eta}{d\xi} = \frac{\nu}{\alpha}(\psi - 1). \qquad [8]$$

In solving the antiforce case problem, in which all quantities including $\kappa$ are positive and $\xi$ is positive backward, we will use the set of non-dimensional variables introduced by Hemmati (1999).

$$\eta = \frac{E}{E_o}, \nu = (\frac{2e\phi}{\varepsilon_o E_o^2})n, \psi = \frac{\nu}{V}, \theta = \frac{T_e k}{2e\phi}, \xi = -\frac{eE_o x}{mV^2},$$
$$\alpha = \frac{2e\phi}{mV^2}, \kappa = -\frac{mV}{eE_o}K, \mu = \frac{\beta}{K}, \omega = \frac{2m}{M}.$$

Also, for antiforce problems for which a large current exists in the vicinity of the shock front, Hemmati's et al. (2011) modified set of fluid-dynamical equations need to be used. The set of electron fluid-dynamical equations describing antiforce waves in non-dimensional form are given as follows:

$$\frac{d}{d\xi}[\nu\psi] = \kappa\mu\nu, \qquad [9]$$

$$\frac{d}{d\xi}[\nu\psi(\psi - 1) + \alpha\nu\theta] = \nu\eta - \kappa\nu(\psi - 1), \qquad [10]$$

$$\frac{d}{d\xi}[\nu\psi(\psi - 1)^2 + \alpha\nu\theta(5\psi - 2) + \alpha\nu\psi - \frac{5\alpha^2\nu\theta}{\kappa}\frac{d\theta}{d\xi}$$
$$+ \alpha\eta^2] = 2\eta\kappa\iota\alpha - \omega\kappa\nu[3\alpha\theta + (\psi - 1)^2], \qquad [11]$$

$$\frac{d\eta}{d\xi} = \kappa\iota - \frac{\nu}{\alpha}(\psi - 1). \qquad [12]$$



https://scholarworks.uark.edu/jaas/vol65/iss1/11
DOI: https://doi.org/10.54119/jaas.2011.6506

Where, $\iota$, is the dimensionless current and is related to the current behind the wave front, $I_1$, by the equation, $\iota = I_1 / \varepsilon_0 K E_0$.

Early on in the study of breakdown waves, the ionization rate was considered to be constant throughout the region in which an electric field is present. Later, some investigators considered it to be a function of temperature only. However, in 1983 Fowler (1983) showed that the assumption of a constant ionization rate was incorrect and therefore replaced it by a computation that was based on free trajectory theory. Fowler's (1983) computation included ionization from both random and directed electron motions within the wave. For ionization in a strong electric field with independent electron drift velocity, Fowler derived an equation for ionization rate. In non-dimensional form Fowler's (1983) expression for the ionization rate is given by

$$\mu = \mu_o \int_{1/\sqrt{2\theta}}^{\infty} \sigma_i z^2 dz \int_B^{\infty} \frac{e^{-(z-u)^2} - e^{-(z+u)^2}}{u} du\, e^{-2Cu}, \quad [13]$$

where $B = (1-\psi)/\sqrt{2\alpha\theta}$ and $C = \kappa\sqrt{2\alpha\theta}/\eta$. This function, which changes from accelerational ionization at the front of the wave to directed velocity ionization in the intermediate stages of the wave, to thermal ionization at the end of the wave, in the case of breakdown waves moving with a slow speed, does remain considerably constant at the beginning of the sheath.

**Boundary Conditions**

Considering the ion number density and velocity behind the wave front to be $N_i$ and $V_i$, behind the wave front the current is

$$eN_iV_i - env = I_1. \quad [14]$$

Absence of an experimentally observed Doppler shift indicates lack of appreciable ion and neutral particle motion in the laboratory frame. Therefore, considering the ion and neutral particle velocities to be almost equal $(V_i \cong V)$, substituting $V$ for $V_i$ and solving equation [14] for $N_i$ results in

$$N_i = \frac{I_1}{eV} + \frac{nv}{V}. \quad [15]$$

For antiforce waves, to find the electron temperature at the shock front, we use the all particle (global) momentum equation, which at the wave front it becomes

$$mnv^2 + nkT_e + MNV^2 + M_iN_iV_i^2 + NkT + N_ikT_i$$

$$+\frac{\varepsilon_0}{2}(E_0^2 - E^2) = MN_0V_0^2 + N_0kT_0.$$

Where, M and N represent the neutral particle mass and number density, T and $T_i$ represent neutral particle and ion temperatures within the sheath region, $N_0, T_0$ and $V_0$ represent the neutral particle number density, temperature and velocity in front of the wave. Considering that at the wave front $V \approx V_i \approx V_0, T \approx T_i = T_0, E \approx E_0$, and also substituting for the variable values at the shock front, the above equation becomes

$$mn_1v_1^2 + n_1kT_{e1} + (MN + M_iN_i - MN_0)V^2 +$$

$$(N + N_i)kT = N_0kT_0.$$

Substituting $N_0$ for $N + N_i$ and m for $M - M_i$ in the above equation, it reduces to

$$mn_1v_1^2 + n_1kT_{e1} - mN_{i1}V^2 = 0.$$

Where, $N_{i1}$ is the ion number density at the wave front and $n_1$, $T_{e1}$ and $v_1$ represent the electron number density, temperature and velocity at the wave front. Substituting for $N_{i1}$ from equation [15] in the above equation reduces it to

$$mn_1v_1(v_1 - V) + n_1kT_{e1} - \frac{mI_1V}{e} = 0.$$

Substituting $\iota$ for $\frac{I_1}{\varepsilon_0 K E_0}$ and the dimensionless variables for antiforce waves in the above equation, gives the electron temperature at the shock front

$$\theta_1 = \frac{\psi_1(1-\psi_1)}{\alpha} - \frac{\kappa\iota}{v_1}. \quad [16]$$

## Results and Discussion

Uman and Mclain (1970) derived expressions relating the stepped leader radiation (electric field intensity or magnetic field flux density) to the leader current. By measuring the radiation field from a distance, they were able to calculate the current by using the derived expression for the stepped leader (proforce wave). Their calculated current values were in the range of 800 to 5000 amperes. However, measuring currents at the lightning channel base and with optical observations, Rakov et al. (1998) report a stepped leader current of 5 kA and a return stroke (antiforce wave) peak current of 10 kA.

Determining K from experimental curves (McDaniel 1964) gives $K/P = 3x10^8$ for helium and $K/P = 4.8x10^7$ for nitrogen at 273 $K$. At a temperature of $10^5$, K will be $2.4x10^9$ for helium and $9x10^9$ for nitrogen and applied fields are usually of the order of $10^5 V/m$. Considering that $E_0, K, \beta$ in our formulas are scaled with P (the electron gas pressure) and using the values of $I_1, \varepsilon_0, E_0, K$ one can estimate the value of $\iota$, which is of the order of one.

In their study of lightning attachment process, Wang et al. (1999) provided evidence of the occurrence of upward discharge making contact with descending leader. They reported that the upward connecting discharge appears to be much weaker in light intensity than its associated downward dart leader. In addition to data on current, Wang et al. (1999) also provided data for upward connecting discharge wave speed, discharge length and leader electric field changes. For upward return stroke, they reported speeds of approximately $2.5x10^8 m/s$.

Using helium-filled screened discharge tubes with different diameters, Asinovsky et al. (1994) performed experimental studies and conducted theoretical analysis of breakdown waves. The theoretical and experimental dependences they obtained, for both positive and negative polarity waves, were in good agreement, indicating the applicability of the ionization drift model to breakdown waves. They reported breakdown wave velocities ranging from $10^7$ m/s to $6x10^7$ m/s.

A trial and error method was utilized to integrate equations 9 through 12. For a given wave speed, α, a set of values for wave constant, κ, electron velocity, $\psi$ , and electron number density, $\nu_1$, at the wave front were chosen. The values of κ, $\psi$ , and $\nu_1$ were repeatedly changed in integrating equations 9 through 12 until the process lead to a conclusion in agreement with the expected conditions at the end of the dynamical transition region of the wave.

For several current values, we were able to integrate the electron fluid-dynamical equations [Equations 9-12] for $\alpha$ value as low as 0.01. $\alpha = 0.01$ represents a wave speed of $0.3x10^8 m/s$ and conforms with the lower experimental speed range for return stroke lightning. The successful solutions required the following boundary values

$\iota = 0.0, \kappa = 1.3, \psi_1 = 0.645, \nu_1 = 0.886$

$\iota = 0.25, \kappa = 1.3, \psi_1 = 0.648, \nu_1 = 0.88$

$\iota = 0.7, \kappa = 1.3, \psi_1 = 0.6564, \nu_1 = 0.88$

$\iota = 1.5, \kappa = 1.3, \psi_1 = 0.674, \nu_1 = 0.847$

$\iota = 2.6, \kappa = 1.3, \psi_1 = 0.68, \nu_1 = 0.83$

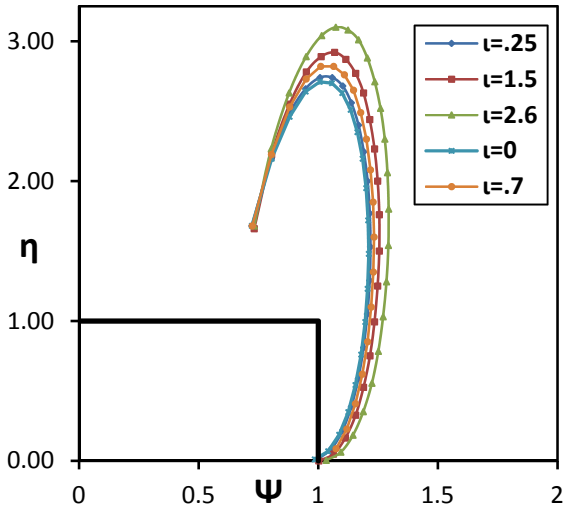


**Figure 1.** Electric field as a function of electron velocity within the sheath region of current bearing antiforce waves for current values of 0, 0.25, .7, 1.5, and 2.6.

Figure 1 represents the dimensionless electric field, η, as a function of dimensionless electron velocity, ψ, within the sheath region of the wave. As the graph confirms, for all current values, the electric field starting from an initial value at the shock front, initially increases within the sheath region; however, as expected by the required boundary conditions, it reduces to a negligible value at the trailing edge of the wave. As the current increases, integration of the set



https://scholarworks.uark.edu/jaas/vol65/iss1/11
DOI: https://doi.org/10.54119/jaas.2011.6506

of equations through the sheath region becomes more difficult and time consuming.

Figure 2 shows the dimensionless electric field, η, as a function of dimensionless position, ξ, within the sheath region of the wave for current bearing antiforce waves.

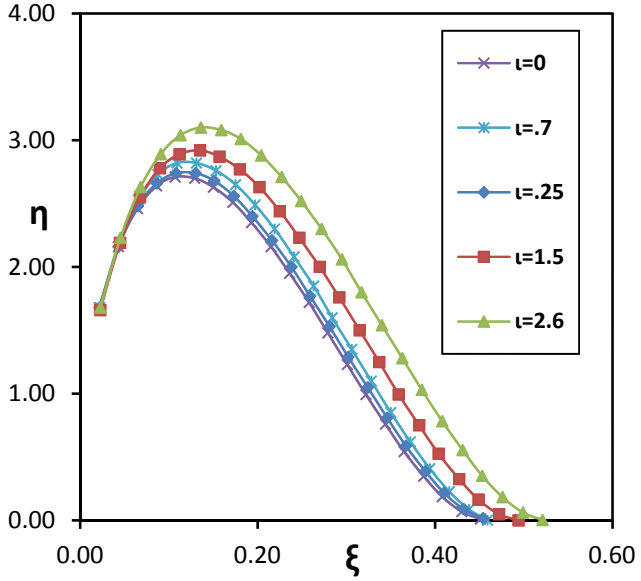


**Figure 2.** Electric field as a function of position with the sheath region of current bearing antiforce waves for current values of 0, 0.25, 0.7, 1.5, and 2.6.

Applying fluid dynamical techniques to the passage of ionizing wave counter to strong electric fields, for wave speed of 10 $m/s$, Sanmann and Fowler's (1975) electric field peaked at a distance of 0.04 m behind the wave front and their total sheath thickness was $0.07m$. As our graphs show, for the wave speed of $3x10^7\ m/s$, our dimensionless sheath thickness is 0.5 which represents an actual sheath thickness of $2.5x10^{-2}\ m$. Measuring electron density behind shock waves, Fujita et al. (2003) report a wave thickness of approximately 5 cm.

Figure 3 depicts the dimensionless electron velocity, ψ, as a function of dimensionless position, ξ, within the sheath region of the wave for antifoce current bearing waves. The graph shows that for all current values, the electron velocity starting from an initial value of less than 1, initially increases; however, for all current values, as expected by the required boundary conditions, reduces to 1 at the end of the sheath region.

Figure 4 represents the dimensionless electron temperature, θ, as a function of dimensionless position, ξ, within the sheath region for antiforce current bearing waves. For all current values, starting from an initial value of approximately 20, the dimensionless electron temperature increases to approximately 67 at the end of the sheath region.

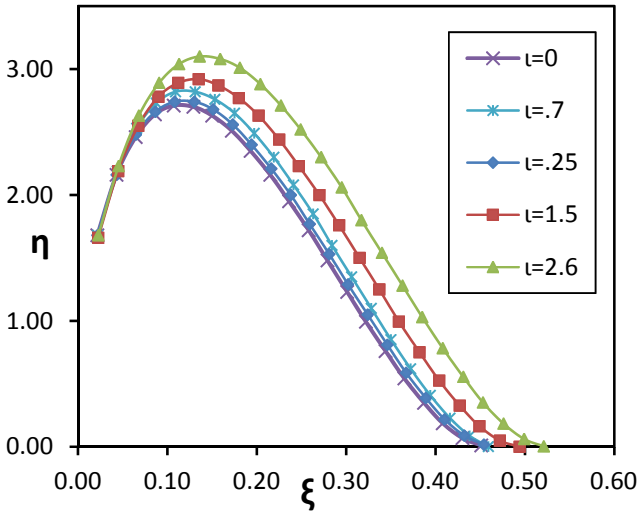


**Figure 3.** Electric field as a function of position with the sheath region of current bearing antiforce waves for current values of 0, 0.25, 0.7, .1.5, and 2.6.

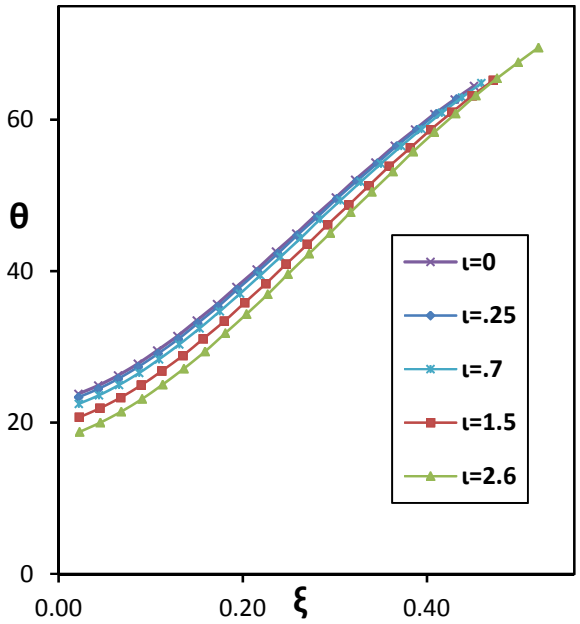


**Figure 4.** Electron temperature as a function of position within the sheath region of current bearing antiforce waves for current values of 0, 0.25, 0.7, 1.5, and 2.6.

For ionizing waves propagating counter to strong electric fields, Sanmann and Fowler (1975) reported that the electron temperature increases rapidly away from the wave front until it reaches a peak value of

around $3.17x10^{7} K$ at a distance of $5.4x10^{-2} m$ behind the wave front. Our results show that the temperature increases behind the shock front and it reaches its maximum dimensionless value of $\theta = 67$ at the trailing edge of the wave. $\theta = 67$ represents electron gas temperature of $3.88x10^{7}$ $K$.

Figure 5 shows the changes in dimensionless electron number density as a function of dimensionless position within the sheath region of the wave. For all current values, starting from an initial value of less than one, the electron number density initially decreases within the sheath; however, it increases as it approaches the trailing edge of the wave.

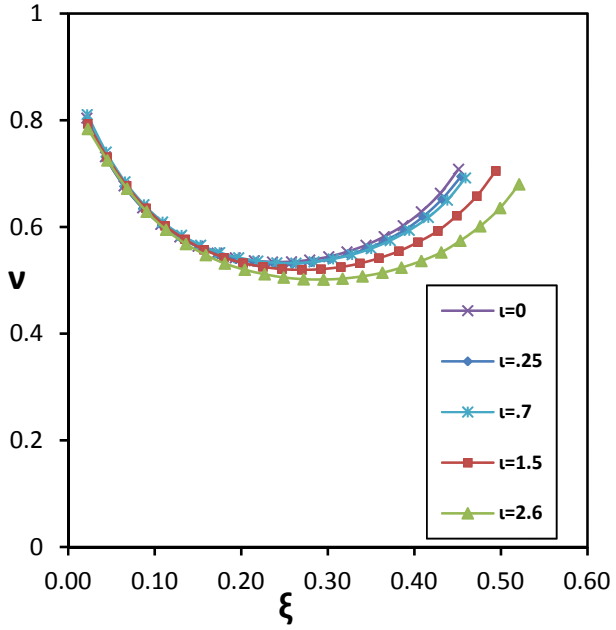


**Figure 5.** Electron number density as a function of position within the sheath region of current bearing antiforce waves for current values of 0, 0.25, 0.7, 1.5, and 2.6.

Using a fluid model, Brok et al. (2003) study the mechanisms responsible for the propagation of the first anode directed ionization wave that occurs in a straight discharge tube during breakdown. Brok et al. (2003) reported peak electron number density of $6x10^{16} / m^{3}$, and an average electron number density of $4x10^{15} / m^{3}$. Our average non-dimensional electron number density of 0.7 represents an actual electron number density of $7.7x10^{15} / m^{3}$ within the sheath region of the wave.

## Conclusions

For a range of dimensionless current values that conform with the experimentally measured current values, using our modified boundary condition on electron temperature, we have been successful in integrating our modified set of electron fluid dynamical equations through the sheath region for antiforce current bearing breakdown waves. For all current values, our solutions meet the expected conditions at the trailing edge of the wave. This is a confirmation of validity of our modified set of electron fluid dynamical equations for antiforce current bearing waves and the set of electron fluid dynamical equations in general.

Providing an accurate mode and an accurate set of equations for breakdown waves is essential for a better understanding of lightning. However, there are many recent applications of breakdown waves in industry and medical sciences which will benefit immensely. An accurate model of breakdown waves, a proper set of equations and solution of the set of equations will be vital for advances in the new applications.

## Acknowledgements

The authors would like to express gratitude for the financial support provided by the Arkansas Space Grant Consortium and the Student Undergraduate Research Fellowship (SURF) program.

## Literature Cited

**Asinovsky EI**, **AN Lagarkov**, **VV Markovets** and **IM Rutkevich**. 1994. On the similarities of electric breakdown waves propagating in shielded discharge tubes. Plasma Sources Science and Technology. 3:556-63.

**Brok WJM**, **J van Dijk**, **MD Bowden**, **JJAM van der Mullen** and **GMW Kroesen**. 2003. A model study of propagation of the first ionization wave during breakdown in a straight tube containing argon. Journal of Physics D: Applied Physics 36:1967-79.

**Fowler RG**. 1983. A trajectory theory of ionization in strong electric fields. Journal of Physics B: Atomic and Molecular Physics 16:4495-510.

**Fowler RG**, **M Hemmati**, **RP Scott** and **S Parsenajadh**. 1984. Electric breakdown waves: Exact numerical solutions. Part I. The Physics of Fluids 27(6):1521-6.



https://scholarworks.uark.edu/jaas/vol65/iss1/11
DOI: https://doi.org/10.54119/jaas.2011.6506

**Fujita K**, **S Sato** and **T Abe**. 2003. Electron density measurements behind shock waves by H-β profile matching. Journal of Thermodynamics and Heat Transfer 17:210-6.

**Haberstich A**. 1964. Ph.D. Dissertation. Experimental and theoretical study of an ionizing potential wave in a discharge tube. University of Maryland, College Park, Maryland.

**Hemmati M**. 1999. Electron shock waves: speed range for antiforce waves. Proceedings of the 22nd International Symposium on Shock Waves; 1999 July 18-23; Imperial College, London, UK. Imperial College 2:995-1000.

**Hemmati M**, **WP Childs**, **H Shojaei** and **DC Waters**. 2011. Antiforce current bearing waves. Proceedings of the 28th International Symposium on Shock Waves (ISSW28), July 2011, England.

**McDaniel EW**. 1964. Collision phenomena in ionized gases. Wiley, New York.

**Paxton GW** and **RG Fowler**. 1962. Theory of breakdown wave propagation. Physical Review 128(3):993-7.

**Rakov VA**, **MA Uman**, **KI Rambo**, **MI Fernandez**, **RJ Fisher**, **GH Schnetzer**, **R Thottappillil**, **A Eybert-Berard**, **JP Berlandis**, **P Lalande** and **A Bonamy**. 1998. New insights into lightning processes gained from triggered-lightning experiments in Florida and Alabama. Journal of Geophysical Research 103(D12):14117-30.

**Sanmann E** and **RG Fowler**. 1975. Structure of electron fluid dynamical plane waves: antiforce waves. The Physics of Fluids 18(11):1433-8.

**Shelton GA** and **RG Fowler**. 1968. Nature of electron fluid dynamical waves. The Physics of Fluids 11(4):740-6.

**Uman MA** and **DK McLain**. 1970. Radiation fields and current of the lightning stepped leader. J Journal of Geophysical Research 75:1058-66.

**Wang D**, **VA Rakov**, **MA Uman**, **N Takagi**, **T Watanabe**, **DE Crawford**, **KJ Rambo**, **GH Schnetzer**, **RJ Fisher** and **ZI Kawasaki**. 1999. Attachment process in rocket-triggered lightning strokes. Journal of Geophysical Research 104(D2):2143-50.